ISSN 0036-0236, Russian Journal of Inorganic Chemistry, 2019, Vol. 64, No. 10, pp. 1309–1316. © Pleiades Publishing, Ltd., 2019.
Russian Text © The Author(s), 2019, published in Zhurnal Neorganicheskoi Khimii, 2019, Vol. 64, No. 10, pp. 1116–1124.

INORGANIC MATERIALS AND NANOMATERIALS

Liquid-Phase Synthesis of Silver Sulfide Nanoparticles in Supersaturated Aqueous Solutions

S. I. Sadovnikov*

Institute of Solid-State Chemistry, Ural Branch, Russian Academy of Sciences, Yekaterinburg, 620990 Russia
**e-mail: sadovnikov@ihim.uran.ru*

Received March 1, 2019; revised April 2, 2019; accepted April 15, 2019

Abstract—Silver sulfide powders and colloidal solutions were synthesized by chemical deposition from aqueous solutions of silver nitrate and sodium sulfide in the presence of sodium citrate as a stabilizing agent. X-ray diffraction, electronic microscopy, the Brunauer–Emmett–Teller method, and dynamic light scattering were used to determine nanoparticle sizes in the deposited powders and colloidal solutions. The varying reagent concentrations in the reaction mixture provided nanopowders with average particle sizes ranging from ~1000 to ~40–50 nm. Silver sulfide nanoparticles in colloidal solutions have sizes of 15–20 nm. A qualitative correlation is found between the silver sulfide particle size and the supersaturation of the solutions used in the synthesis.

Keywords: chemical deposition, supersaturation, nanoparticles, silver sulfide

DOI: 10.1134/S0036023619100115

INTRODUCTION

Sulfide semiconductors are known to change their physical and chemical properties when their particle sizes are reduced to the nanometer scale. The size effect in semiconductors is the manifested most strongly in their electronic properties when the particle size becomes smaller than the exciton size [1]. Not only extensive studies of nanocrystalline silver sulfide Ag_2S are now underway [2–5], just as for ZnS, CdS, PbS, Cu_2S, and Hg_2S [6–10], but it has already found application. This is due to an option to modify the properties of Ag_2S, especially electronic and optical properties, by changing nanoparticle (crystallite) sizes.

Bulk silver sulfide with particle sizes greater than 500 nm is a semiconductor with the bandgap E_g ~ 0.88–0.90 eV at 300 K [11]. According to [12], the decreasing particle sizes of silver sulfide broaden the bandgap, and the E_g of Ag_2S nanoparticles sized ~ 8 nm is 2.85 eV.

Nanocrystalline silver sulfide can be prepared by various chemical and physical methods. According to [13], bottom–up approach syntheses are the best for preparing nanostructured silver sulfides. Of them, chemical deposition from aqueous solutions is regarded to be efficient for preparing nanocrystals with tailored sizes and a small size variance [14–16]. Sulfides Ag_2S, CdS, Cu_2S, Hg_2S, PbS, ZnS are nearly water-insoluble (their solubility products range from 10^{-24} to 10^{-50}), so the aqueous solutions useful for the deposition of sulfides, including Ag_2S, are, as a rule, supersaturated in the sulfide. However, a correlation between the supersaturation and Ag_2S nanoparticle size has yet not been discussed anyhow.

In this paper, we systematize the hydrochemical deposition parameters to prepare silver sulfide in the form of nanocrystalline powders and colloidal solutions with various nanoparticle sizes, and we are the first to match the silver sulfide nanoparticle size and the supersaturation of the reaction mixture used in the synthesis.

EXPERIMENTAL

Powders and colloidal solutions of silver sulfide Ag_2S were prepared by chemical deposition from aqueous solutions of silver nitrate $AgNO_3$, sodium sulfide Na_2S, and sodium citrate $Na_3C_6H_5O_7$ (Na_3Cit). The synthesis was carried out at 298 K in the dark. Sodium citrate does not form complexes with silver, but in the synthesis it plays the role of a stabilizing agent to prevent nanoparticle growth. Sodium citrate is an electrostatic stabilizing agent. Citrate ion $C_6H_5O_7^{3-}$ has three negatively charged oxygen ions O^-. When citrate is added to an aqueous solution containing silver sulfide particles, citrate ions are attached to particle surfaces via one O^- ion, while the other two of the negatively charged ions are directed inward the solution. As a result, every silver sulfide particle is surrounded by a negatively charged citrate layer, and this

layer keeps sulfide particles from coming together and stabilizes their sizes [17–19].

Since sodium citrate in aqueous solutions with low S^{2-} ion concentrations can reduce Ag^+ ions to form silver metal nanoparticles, for depositing Ag-free silver sulfide we used reaction mixtures with a small relative excess of sodium sulfide Na_2S. The deposition of nanocrystalline silver sulfide occurred in the dark in a neutral medium at pH ~ 7 by the following reaction scheme:

$$2AgNO_3 + Na_2S \xrightarrow{Na_3C_6H_5O_7} Ag_2S\downarrow + 2NaNO_3. \quad (1)$$

To obtain Ag-free colloidal solutions and nanopowders, we carried out the synthesis with a small excess ($0.01 \geq \delta \geq 0.5$) of sodium sulfide; that is, if reaction (1) is written with stoichiometric coefficients, there were $(1 + \delta)$ Na_2S molecules, instead of one, per every two $AgNO_3$ molecules. So, the sulfide ion S^{2-} and silver ion Ag^+ concentrations in the synthesis were related as $C_{S^{2-}} = (1 + \delta)C_{Ag^+}/2$.

The pH in solutions was monitored on an Hanna Instruments™ HI73127 ion meter. Bidistilled water (pH 6.7–6.9) was used to prepare the initial solutions and to synthesize nanoparticles. Reagent concentrations in the synthesis of colloidal silver sulfide solutions are so low that the pH change in aqueous solutions relative to the neutral solvent (water) falls within the measurement error of the ion meter.

Beforehand prepared and fully equilibrated aqueous solutions of $AgNO_3$, Na_2S, and Na_3Cit were used in the synthesis. First, to 50 mL of the silver nitrate solution, added was 50 mL of the sodium citrate (stabilizer) solution; then, the thus-prepared solution was mixed with 100 mL of the Na_2S solution. Since the reagents were combined, the reaction mixture darkened rapidly (in several seconds), indicating the formation of a silver sulfide supersaturated solution. Then, Ag_2S particles settled down, and in 30–60 min solution became clear. For complete sulfiding to be provided, the deposit was allowed to stand in contact with the solution for 24 h. The deposited Ag_2S powder was at least four times washed with distilled water by decantation, filtered, and then air-dried at 323 K.

Nanocrystalline Ag_2S powders with particles sizes ≤60 nm were deposited from reaction mixtures where the $AgNO_3$ and Na_2S concentrations were 50 and 25 mmol/L, respectively (Table 1). Na_3Cit concentrations varied from 5 to 100 mmol/L. The increasing Na_3Cit concentrations decreased Ag_2S particle sizes. We failed to deposit an Ag_2S nanopowder with particle sizes less than 20 nm, due to ≤20-nm nanoparticles forming a stable colloidal solution and not settling for several years. Such the stable colloidal silver sulfide solutions were prepared from reaction mixtures **8**–**19** where the silver nitrate was ≤2.5 mmol/L.

The X-ray diffraction measurements of deposited powders were in the angle range $2\theta = 20°–95°$ with the step $\Delta(2\theta) = 0.02°$ on a Shimadzu XRD-7000 diffractometer using $CuK_{\alpha1,2}$ radiation. The exposure time per point was 10 s. The structure of the prepared silver sulfide powders was refined in the X'Pert HighScore Plus program package [20]. The average particle size D (more exactly, the average coherent scattering length) in the prepared silver sulfide nanopowders was found by the Williamson–Hall method from the broadening of diffraction reflection, using the relationship between the normalized reflection broadening $\beta^*(2\theta) = [\beta(2\theta)\cos\theta]/\lambda$ and the scattering vector $s = (2\sin\theta)/\lambda$ [21, 22]. In order to determine the broadening $\beta(2\theta)$, the experimentally measured full width at half-maximum $FWHM_{exp}$ of each diffraction reflection was compared to the instrumental resolution function of the diffractometer preliminarily measured on a reference lanthanum hexaboride LaB_6 sample (NIST Standard Reference Powder 660a; the unit cell period $a = 0.415692$ nm). In a well-annealed homogeneous bulk LaB_6 powder with the average particle size 5 μm, there are no reasons (such as small particle sizes, microstresses, and nonhomogeneity) that would have caused the physical broadening of diffraction reflections, and the instrumental broadening of diffraction reflections is only observed in it.

The instruments used to study the microstructure, particle size, and elemental chemical composition of Ag_2S powders were a JEOL-JSM LA 6390 scanning electron microscope (SEM) equipped with a JED 2300 Energy Dispersive X-ray (EDX) Analyzer and a JEOL JEM-2010 transmission electron microscope, the letter used to record transmission electron microscopic (TEM) images in order for determining silver sulfide nanoparticle sizes in colloidal solutions.

The elemental chemical composition of the prepared silver sulfide powders was also determined by X-ray fluorescence spectroscopy (XPS) on an S4 EXPLORER (Bruker) X-ray fluorescence analyzer. All measurements were carried out in vacuo in the high-sensitivity mode with automatically selected radiation filters. The test samples were pellets 18 mm in diameter pressed of test powders on a Licowax C micropowder amide wax substrate. The silver and sulfur as the major elements were quantified from the intensities of the $AgK_{\alpha1}$ and $SK_{\alpha1}$ lines with the binding energies 22.16292 and 2.30784 keV and the $K_{\alpha2}$ and $K_{\beta1}$ lines of silver and sulfur. The other elements were quantified from the intensities of their respective lines $K_{\alpha1}$, $K_{\alpha2}$, and $K_{\beta1}$.

The average particle size of Ag_2S was also estimated from S_{sp}, the specific surface area of the prepared powder, as $D = 6/\rho S_{sp}$ ($\rho = 7.25$ g/cm^{-3} is the silver sulfide density). The specific surface area was found experimentally by the Brunauer–Emmett–Teller (BET) method on a Gemini VII 2390t Surface Area Analyzer.

Table 1. Reaction mixtures, specific surface areas S_{sp} of powders, and average particle sizes D in silver sulfide powders and colloidal solutions

Silver sulfide	No.	Concentration in the reaction mixture, mmol /L			S_{sp}, m^2/g	D, nm			
						in deposited powders		in colloidal solutions	
		$AgNO_3$	Na_2S	Na_3Cit		BET	X-rays	DLS	TEM
Bulk powder	1	50	200	0	0.82 ± 0.02	1008	–	–	–
	2	50	500	5	1.6 ± 0.1	515	–	–	–
	3	50	100	25	1.9 ± 0.1	430	–	–	–
	4	50	50	100	5.1 ± 0.1	163	85 ± 7	–	–
Nanoparticles	5	50	25.5	12.5	14.9 ± 0.2	56 ± 5	46 ± 8	55 ± 10	–
	6	50	25.4	25	19.0 ± 0.2	44 ± 5	43 ± 6	60 ± 10	–
	7	50	25.1	100	15.6 ± 0.2	53 ± 5	49 ± 8	66 ± 10	–
Quantum dots	8	0.3125	0.165	5	–	No deposite		2.3 ± 1	2–3
	9	0.3125	0.168	2.5	–	″		2.7 ± 1	2–3
	10	0.3125	0.170	1	–	″		3.1 ± 1	2–4
	11	0.625	0.313	5	–	″		4.2 ± 2	3–4
	12	0.625	0.325	3.75	–	″		5.6 ± 2	5–6
	13	2.5	1.30	1	–	″		8.0 ± 2	8–10
	14	1.25	0.635	1.25	–	″		8.2 ± 2	8–10
	15	0.625	0.330	2.5	–	″		9.2 ± 2	8–10
	16	0.625	0.335	1.25	–	″		10.0 ± 2	9–11
	17	2.5	1.35	2.5	–	″		15.0 ± 3	11–12
	18	0.625	0.350	15	–	″		16.0 ± 4	10–12
	19	1.25	0.630	7.5	–	″		17.0 ± 5	12–15

The Ag_2S nanoparticle size D was determined immediately in colloidal solutions by dynamic light scattering (DLS) on a Zetasizer Nano ZS (Malvern Instruments) particle size analyzer at 298 K using a He–Ne laser. At least three replica particle size measurements were done in each solution.

RESULTS AND DISCUSSION

The silver and sulfur in silver sulfide powders as measured by XPS amount to 79.5 ± 0.5 and 12.0 ± 0.5 wt %, respectively, and these values correspond to $Ag_{2.00 \pm 0.06}S_{1.00 \pm 0.03}$ (Fig. 1). The prepared powders also contain 0.3 to 0.5 wt % Na, whose source is the sodium citrate Na_3Cit adsorbed on the surface of sulfide powders, and ~7.5 wt % impurity oxygen, also adsorbed on the surface of sulfide powders. Long-term high-vacuum annealing of powders decreased the adsorbed oxygen to 1.5–2.0 wt %.

The X-ray diffraction patterns of powders deposited from reaction mixtures **2** and **6** (Table 1) shown in Fig. 2 exemplify the patterns of silver sulfide Ag_2S powders. The particle sizes D of bulk powders **1**–**3** were found from the measured surface areas S_{sp}, which ranged from ~0.82 to ~1.61 m^2/g. X-ray diffraction pattern *2* in Fig. 2 was used in crystal structure refinement for bulk powders. From the quantitative refinement of X-ray diffraction pattern *2* and a comparison with reported data [23], it flows that the observed diffraction reflections correspond to the single-phase monoclinic (space group $P2_1/c$) stoichiometric silver sulfide having the acanthite α-Ag_2S structure. The unit cell parameters of bulk monoclinic acanthite α-Ag_2S as derived from experimental diffraction data are a = 0.42264(2) nm, b = 0.69282(3) nm, c = 0.95317(3) nm, β = 125.554(2)°.

The Ag and S contents of an air-dried bulk silver sulfide powders having the average particle size ~500 nm as probed by EDX are 86.8 ± 0.4 and 12.9 ± 0.1 wt %, respectively. This values correspond to stoichiometric Ag_2S within the measurement error and agree with XPS data.

The X-ray diffraction patterns of silver sulfide nanopowders having average particle sizes from ~40 to ~50 nm, deposited from reaction mixtures **5**, **6**, and **7**, are similar to one another. These patterns are exemplified by the X-ray diffraction pattern of nanopowder **6** shown in Fig. 2. The quantitative refinement of the

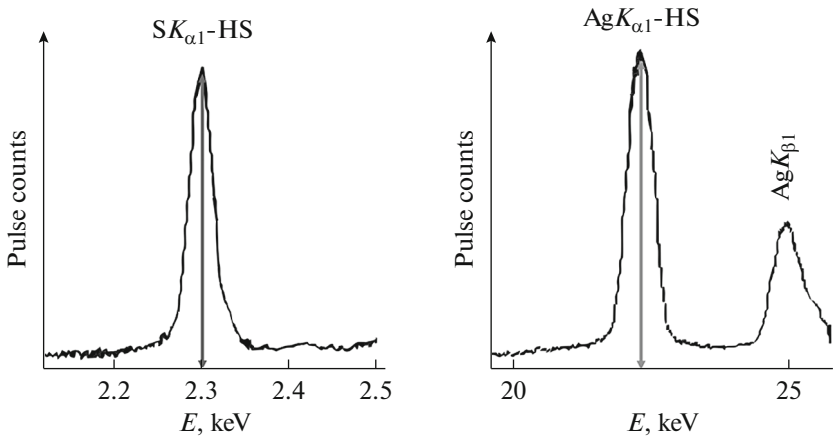

Fig. 1. X-ray fluorescence analysis of silver sulfide nanopowders. The lines S$K_{\alpha1}$ and Ag$K_{\alpha1}$ were recorded in the high-sensitivity mode with a CuLiF200 filter. The intensities and energies are on the logarithmic scale.

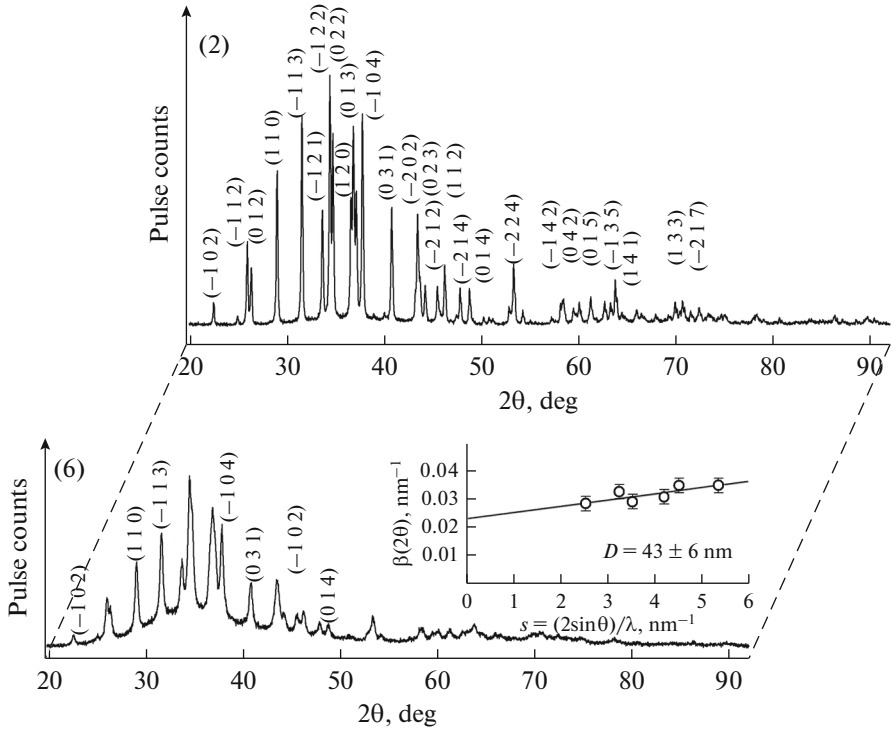

Fig. 2. X-ray powder diffraction patterns of silver sulfide powders deposited from reaction mixtures **2** and **6** (Table 1). Bulk powder **2** having the average particle size ~500 nm has the Ag_2S stoichiometry. Nanopowder **6** having the average particle size ~43 nm is nonstoichiometric and has the composition ~$Ag_{1.93}S$. Both powders have an acanthite-type monoclinic structure (space group $P2_1/c$). X-ray diffraction patterns are recorded using Cu$K_{\alpha1,2}$ radiation.

X-ray diffraction patterns of nanopowders took into account the varying occupancies of crystallographic positions for silver and sulfur atoms, so the convergence was noticeably enhanced. Structure refinement for silver sulfide nanopowders in comparison to the reported values [24] implies that the observed set of diffraction reflections corresponds to monoclinic (space group $P2_1/c$) silver sulfide, the Ag and S atomic coordinates and unit cell parameters of the nanopowders being close to the respective values for bulk Ag_2S. However, the 4*e* site occupancy for the atoms Ag(1) and Ag(2) in nanopowders appeared to be slightly less than unity. For nanopowder **6**, in particular, the 4e site occupancy for the atoms Ag(1) and Ag(2) is ~0.97 and ~0.96, respectively. This means that silver sulfide nanoparticles with sizes smaller than ~50–60 nm have vacant sites in the metal sublattice, are nonstoichiometric, and their composition is ~$Ag_{1.93}S$. The Riet-

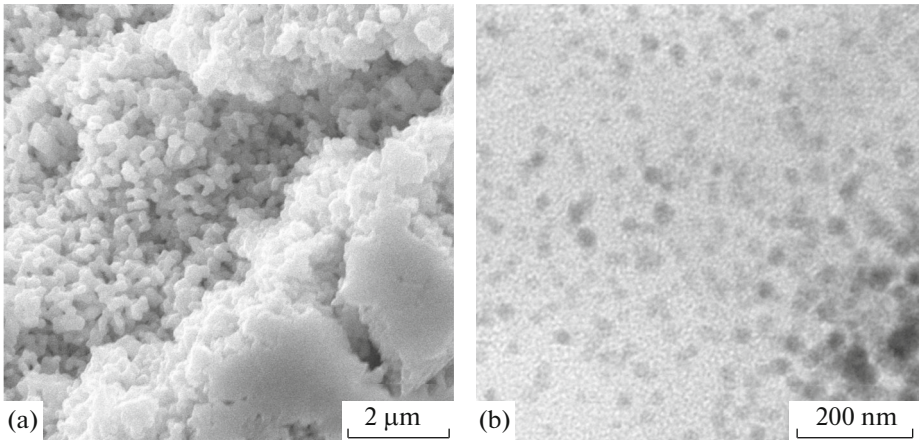

Fig. 3. (a) SEM image of bulk powder **2** and (b) TEM image of silver sulfide nanopowder **5**.

veld convergence factors were R_I (R_B) = 0.0555, R_p = 0.1165, and ωR_p = 0.1431. According to the calculations, a $Ag_{1.93}S$ nanocrystalline powder has a monoclinic (space group $P2_1/c$) acanthite-type structure with the following unit cell parameters: a = 0.4234(3) nm, b = 0.6949(3) nm, c = 0.9549(5) nm, β = 125.43(6)°. One can see that the unit cell parameters of bulk and nanocrystalline monoclinic silver sulfides only slightly differ from each other.

The refinement of X-ray diffraction patterns showed that the nanopowders are nonstoichiometric and have compositions ranging from $Ag_{1.93}S$ to $Ag_{1.97}S$. The diffraction reflections of the nanopowders are broadened, so closely spaced reflections are overlapping. The inset to the X-ray diffraction pattern of nanopowder **6** shows the average coherent scattering length sizes D as evaluated from the broadening of nonoverlapping diffraction reflections (−1 0 2), (1 1 0), (−1 1 3), (−1 0 4), (0 3 1), and (0 1 4). According to this evaluation, the average nanoparticle size D in nanopowder **6** is 43 ± 6 nm. Similar evaluation gives the values of 46 ± 8 and 49 ± 8 nm for the average nanoparticle sizes D in silver sulfide nanopowders **5** and **6**, respectively. The silver sulfide nanoparticle sizes derived from diffraction reflection broadening agrees with the BET estimates of particle sizes (Table 1).

The BET and X-ray diffraction estimates of average particle sizes are verified by electron microscopic data. Figure 3 shows a SEM image of bulk powder **2** and a TEM image of nanopowder **5**. The particle sizes in bulk powder **2** are 400–500 nm, and in nanopowder **5**, from 40 to 60 nm.

The Ag_2S nanoparticle sizes in colloidal solutions **8**–**19** as probed by DLS do not exceed 20 nm (Fig. 4), and these nanoparticles may be treated as quantum dots, i.e., as particles whose semiconductor properties can feature quantum size effects.

The TEM images of colloidal solutions **13** and **17** shown in Fig. 5 by the way of example, as well as the nanoparticle sizes listed in Table 1 (derived from TEM images), support the results of DLS particle size measurements.

In the direct transmitted light the prepared colloidal solutions are whity brown and completely transparent, but when viewed from the side, they look semitransparent and bluish, signifying their opalescence. The observed opalescence of a solution is a consequence of density fluctuations on which the light is scattered and which arise from the absence of small (<20 nm) particles in the solution.

The stability of the prepared colloidal solutions can be elucidated by measuring the ζ potential of nanoparticles in the solution. The signature of an electrostatic stability of a colloidal solution is the absolute value of the ζ potential falling within the range from −35 ± 15 to +35 ± 15 mV. The DLS measurements of the ζ potential and particle sizes of the nanoparticles showed that, in 3 days after solutions **8**–**19** were pre-

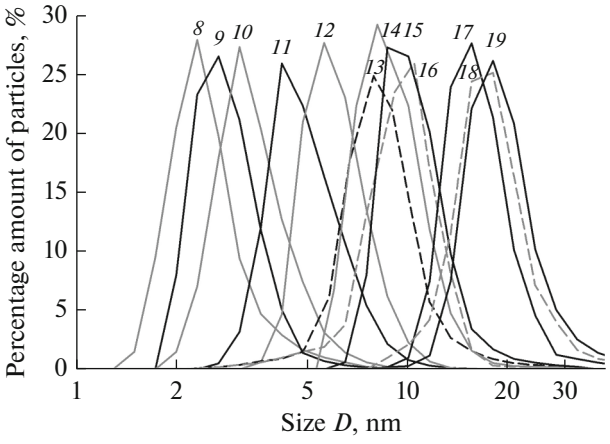

Fig. 4. Silver sulfide particle size distribution in colloidal solutions **8**–**19** as measured by DLS (Table 1). Size D is on the logarithmic scale.

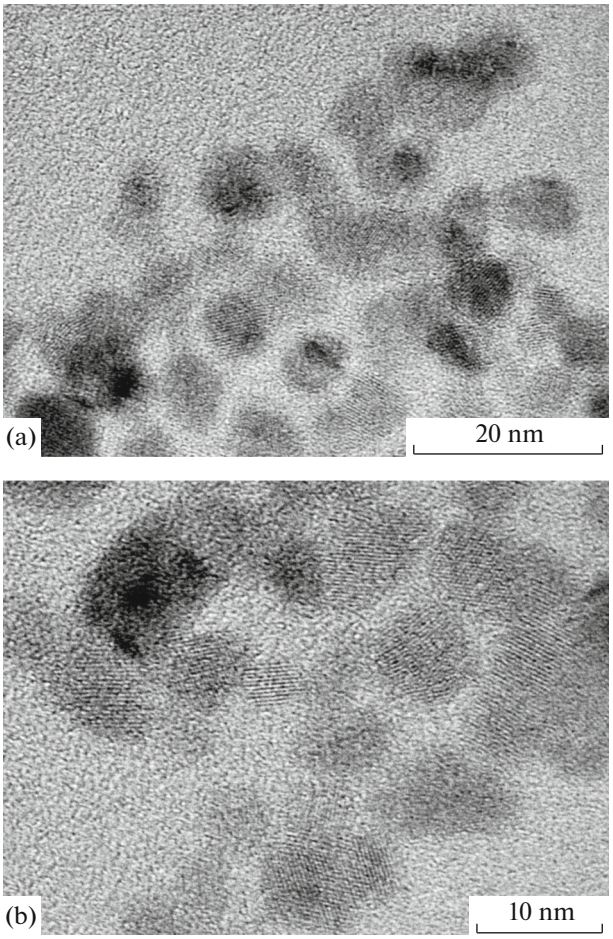

Fig. 5. TEM image of colloidal solutions (a) 17 and (b) 13 (Table 1).

pared, their ζ potentials ranged from −45 to −28 mV and nanoparticle sizes were 2–13 nm. In 100 days after the synthesis, both the ζ potential and Ag_2S nanoparticle size remained nearly unchanged. The great negative values of the ζ potential in colloidal solutions **8**–**19** and their weak variations upon long-term storage prove the stability of these solutions.

Silver sulfide Ag_2S has one of the least values of solubility product K_{sp}, equal to 6.3×10^{-50} at 298 K [25, 26]. This is about 10^{23-28} times lower than any one of the solubility products of cadmium, lead, and zinc sulfides, which are 7.9×10^{-27}, 2.5×10^{-27}, and 2.5×10^{-22}, respectively [25]. With this negligible solubility, Ag_2S deposition occurs very rapidly, in few seconds, given a sufficient Na_2S concentration in the batch.

Silver sulfide formation is possible and indeed occurs if its ion product $IP = a^2_{Ag^+}a_{S^{2-}} = \gamma^2_{Ag^+}C^2_{Ag^+}\gamma_{S^{2-}}C_{S^{2-}}$ is greater than the solubility product K_{sp}. It is due to the small value of the solubility product that the batches used to prepare powders and colloidal solutions with silver sulfide quantum dots are supersaturated in silver sulfide. The supersaturation Δ_{ss}, whose value characterizes the excess of the ion product of a compound over its solubility product, is determined as

$$\Delta_{ss} = IP/K_{sp} = \gamma^2_{Ag^+}C^2_{Ag^+}\gamma_{S^{2-}}C_{S^{2-}}/K_{sp}. \quad (2)$$

When the ionic strength I in the solution is greater than zero ($I > 0$), ion product calculations should take into account the activity coefficients γ_i of the respective ions. A model taking into account ionic interactions can be found in [27]. It is shown therein that coefficients γ_i are presented as

$$\ln\gamma_i = \ln\gamma_i^{DH} + \sum_j \varepsilon_{i,j}(I)m_j + \sum_j\sum_k c_{ijk}m_jm_k + \ldots, \quad (3)$$

where m is molal concentration, $\ln\gamma_i^{DH} \sim -z_i^2AI^{1/2}$, γ_i^{DH} is the activity coefficient obtained from the Debye–Hückel equation, z_i is the ion charge, A is a constant; $\varepsilon_{ij}(I)$, and c_{ijk} stands for decomposition coefficients, the first being dependent on, and the second independent of, the ionic strength of the solution. For most ions, however, $\varepsilon_{ij}(I)$ and c_{ijk} are unknown, so Eq. (3) is actually inapplicable for estimating activity coefficients.

The activity of silver ions, i.e., the fraction of uncomplexed silver ions that are capable of reacting with sulfur ions, may be estimated using the instability constants of silver species. The analytical chemistry reference books, either in Russia or abroad, are silent about complexation between silver ions and citrate ions. In aqueous solutions, however, silver forms mono-, di-, and trihydroxo complexes Ag(OH), $Ag(OH)_2^{1-}$, and $Ag(OH)_3^{2-}$, whose instability constants K ($pK = -\log K$) are $K_{11} = \dfrac{[Ag(OH)]}{[Ag^+][OH^-]} = 5 \times 10^{-3}$, $K_{12} = \dfrac{[Ag(OH)_2^{1-}]}{[Ag^+][OH^-]^2} = 1 \times 10^{-4}$, and $K_{13} = \dfrac{[Ag(OH)_3^{2-}]}{[Ag^+][OH^-]^3} = 6.3 \times 10^{-6}$ ($pK_{11} = 2.3$, $pK_{12} = 4.0$, and $pK_{13} = 5.2$) [25]. The appearance of hydroxo complexes reduces the amount of free Ag^+ ions in the solution. If $C_{Ag,\Sigma} = [Ag^+] + [Ag(OH)] + [Ag(OH)_2^{1-}] + [Ag(OH)_3^{2-}]$ is the overall concentration of all soluble silver species (free silver ions and silver hydroxo complexes), then after simple transformations with account to instability constants, it will be

$$C_{Ag,\Sigma} = [Ag^+]\{1 + K_{11}[OH^-] + K_{12}[OH^-]^2 + K_{13}[OH^-]^3\}. \quad (4)$$

$[OH^-] = [H^+] = 10^{-7}$ in a neutral medium, so replacing $[OH^-]$ in (4) by $[H^+]$, we obtain, in accor-

dance with (4), the silver ion concentration $[Ag^+]$ involved in Ag_2S formation as

$$[Ag^+] = \frac{C_{Ag,\Sigma}}{1 + K_{11}[H^+] + K_{12}[H^+]^2 + K_{13}[H^+]^3}. \quad (5)$$

Since the deposition of nanocrystalline silver sulfide occurs in a neutral medium at pH 7, from Eq. (5) we arrive at $[Ag^+] = C_{Ag^+} \approx C_{Ag,\Sigma}$.

Sulfur ions exist in aqueous solutions in the form of S^{2-}, HS^-, and H_2S. According to the ion equilibrium diagram in the S^{2-}–H_2O system, which is available in the electronic form [28], the fractional concentration $C_{S^{2-}}$ of S^{2-} ions in the region of pH 7 is ~0.01 of the $c_{S,\Sigma}$.

Silver does not form citrate complexes, so we used reference values of activity coefficients in Eq. (2) of this work to go from concentrations C_{Ag^+} and $C_{S^{2-}}$ to the activities of free ions Ag^+ and S^{2-}.

The ionic strength of the used solutions, estimated as $I = \frac{1}{2}\sum_i C_i z_i^2$, where c_i is the concentration of the ith ion, varies only weakly, from 0.03 to 0.12, and averages ~0.1. The activity coefficients at this ionic strength are $\gamma_{Ag^+} = 0.75$ and $\gamma_{S^{2-}} = 0.38$ [25].

The supersaturations Δ_{ss} calculated from Eq. (2) with $C_{Ag^+} \approx C_{Ag,\Sigma}$, $C_{S^{2-}} \approx 0.01C_{S,\Sigma}$, $\gamma_{Ag^+} = 0.75$, and $\gamma_{S^{2-}} = 0.38$, are approximates, but they qualitatively show the effect of supersaturation on the particle sizes of silver sulfide powders and colloidal solutions. Figure 6 shows a particle size (D) versus supersaturation (Δ_{ss}) plot for silver sulfide powders and colloidal solutions (supersaturation is on the logarithmic scale). Despite a great scatter, the silver sulfide particle size evidently increases with rising supersaturation in the reaction mixture.

The effect on silver sulfide particle sizes caused by the sodium citrate concentration as a stabilizing agent is well-defined in colloidal solutions where the $AgNO_3$ concentration is fixed and the sodium citrate concentration is variable. In solutions **11**, **12**, **15**, and **16** (Table 1), for example, a reduction in Na_3Cit concentration from 5 to 3.75, 2.5, and 1.25 mmol/L leads to a rise in quantum dots from 4.2 to 5.6, 9.2 and 10.0 nm, respectively, due to the decreasing stabilizing effect of sodium citrate. The same is observed in colloidal solutions **8**, **9**, and **10**. Thus, in the range $C_{Na_3Cit} \le 5$ mmol/L, the increasing sodium citrate amount in the reaction mixture favors the synthesis of smaller silver sulfide particle sizes.

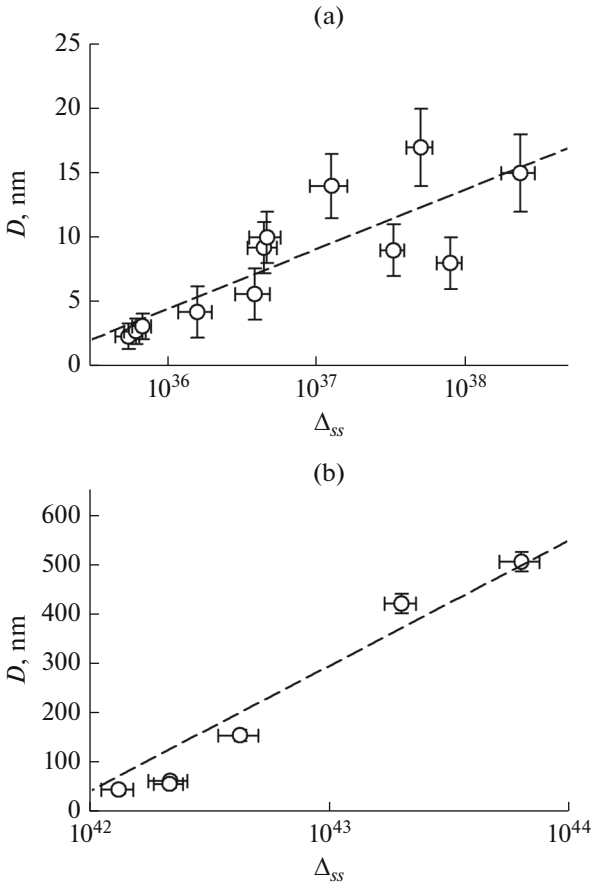

Fig. 6. Silver sulfide particle size in (a) colloidal solutions and (b) powders versus supersaturation Δ_{ss} in the reaction mixture (supersaturation Δ_{ss} is on the logarithmic scale).

CONCLUSIONS

Single-phase silver sulfide powders having the acanthite-type (α-Ag_2S) monoclinic structure (space group $P2_1/c$) have been deposited from aqueous solutions of silver nitrate, sodium sulfide, and sodium citrate. A gradually change in the ratio between reagent concentrations offers a means for depositing Ag_2S particles with the tailored average sizes ranging from ~1000 to 40–50 nm. Silver sulfide with particle sizes greater than 100 nm has the Ag_2S stoichiometry. Nanocrystalline silver sulfide with particle sizes smaller than 60 nm contains structural vacancies in the metal sublattice; that is, it is nonstoichiometric and its composition is $Ag_{1.93-1.97}S$.

Aqueous colloidal solutions of silver sulfide quantum dots having sizes from 2–3 to 15–20 nm remain stable for more than three years.

The particle size in silver sulfide powders and colloidal solutions is related to the supersaturation of reaction mixtures in silver and sulfur ions. At low concentrations, the increasing sodium citrate amount in the reaction

mixture stabilizes nanoparticles and favors the synthesis of smaller silver sulfide particle sizes.

ACKNOWLEDGMENTS

The author is grateful to Professor V.F. Markov for fruitful discussion.

FUNDING

The study was financially supported by the Russian Science Foundation (project No. 19-73-20012) in the Institute of Solid-State Chemistry of the Russian Academy of Sciences, Ural Branch.

REFERENCES

1. H.-E. Schaefer, *Nanoscience.* The Science of the Small in Physics, Engineering, Chemistry, Biology and Medicine (Springer, Heidelberg/Dordrecht/New York, 2010). https://doi.org/10.1007/978-3-642-10559-3
2. A. Tang, Yu. Wang, H. Ye, et al., Nanotecnology **24**, 355602 (2013).
3. S. I. Sadovnikov and A. I. Gusev, J. Mater. Chem. A **5**, 17676 (2017).
4. S. I. Sadovnikov, A. A. Rempel, and A. I. Gusev, Russ. Chem. Rev. **87**, 303 (2018). https://doi.org/10.1070/RCR4803
5. Y. Zhang, Y. Liu, C. Li, et al., J. Phys. Chem. C **118**, 4918 (2014). https://doi.org/10.1021/jp501266d
6. S. Goel, F. Chen, and W. Cai, Small **10**, 631 (2013). https://doi.org/10.1002/smll.201301174
7. X. Shi, S. Zheng, W. Gao, et al., J. Nanopart. Res. **16** (12), 2741 (2014). https://doi.org/10.1007/s11051-014-2741-3
8. S. I. Sadovnikov, A. I. Gusev, and A. A. Rempel, Russ. Chem. Rev. **85**, 731 (2016). https://doi.org/10.1070/RCR4594
9. S. I. Sadovnikov and A. I. Gusev, J. Alloys Compd. **610**, 196 (2014). http://dx.doi.org/10.1016/j.jallcom.2014.04.220
10. H. Y. Hoang, R. M. Akhmadullin, F. Yu. Akhmadullina, et al., Russ. J. Inorg. Chem. **63**, 256 (2018). https://doi.org/10.1134/S0036023618020109
11. P. Junod, Helv. Phys. Acta **32**, 567 (1959).
12. R. Chen, N. T. Nuhfer, L. Moussa, et al., Nanotecnology **19**, 455604 (2008). https://doi.org/10.1088/0957-4484/19/45/455604
13. A. A. Rempel, Russ. Chem. Rev. **76**, 435 (2007). https://doi.org/10.1070/RC2007v076n05ABEH003674
14. V. F. Markov, L. N. Maskaeva, and P. N. Ivanov, *Hydrochemical Deposition of Metal Sulfide Films: Modeling and Experiment* (Izd–vo UrO RAN, Yekaterinburg, 2006) [in Russian]. ISBN 5-7691-1766-4.
15. S. G. Kwon and T. Hyeon, Acc. Chem. Res. **41**, 1696 (2008).
16. G. P. Panasyuk, I. V. Kozerozhets, E. A. Semenov, et al., Russ. J. Inorg. Chem. **63**, 1303 (2018). https://doi.org/10.1134/S0036023618100157
17. R. Chen, N. T. Nuhfer, L. Moussa, et al., Nanotecnology **19**, 455604 (2008). https://doi.org/10.1088/0957-4484/19/45/455604
18. S. Xiong, B. Xi, K. Zhang, et al., Sci. Rep. **3**, 2177 (2013). https://doi.org/10.1038/srep02177
19. W. Zhang, L. Zhang, Z. Hui, et al., Solid. State Ionics **130**, 111 (2000). https://doi.org/10.1016/S0167-2738(00)00497-5
20. X'Pert HighScore Plus. Version 2.2e (2.2.5) (PANalytical, Almedo, the Netherlands).
21. G. K. Williamson and W. H. Hall, Act. Metal. **1**, 22 (1953).
22. A. I. Gusev, *Nanomaterials, Nanostructures, Nanotechnologies* (Fizmatlit, Moscow, 2009) [in Russian]. ISBN 978-5-9221-0582-8.
23. S. I. Sadovnikov, A. I. Gusev, and A. A. Rempel, Superlatt. Microstr. **83**, 35 (2015). doi.org/ https://doi.org/10.1016/j.spmi.2015.03.024
24. S. I. Sadovnikov, A. I. Gusev, and A. A. Rempel, Phys. Chem. Chem. Phys. **17**, 12466 (2015). https://doi.org/10.1039/C5CP00650C
25. Yu. Yu. Lur'e, *The Analytical Chemistry Handbook* (Khimiya, Moscow, 1967) [in Russian].
26. P. Patnaik, *Dean's Analytical Chemistry Handbook* (McGraw-Hill, New York, 2004). ISBN: 978-0071410601
27. *Activity Coefficients in Electrolyte Solutions*, Ed. by K. S. Pitzer (CRC, Boca Raton, 1991), p. 75.
28. www.novedu.ru/calc/fm-s.htm.

Translated by O. Fedorova